Liu *et al. Stem Cell Research & Therapy* (2024) 15:248
https://doi.org/10.1186/s13287-024-03861-7

Stem Cell Research & Therapy

RESEARCH Open Access

Cxcl10 and *Cxcr3* regulate self-renewal and differentiation of hematopoietic stem cells

Fangshu Liu[1], Xiaofan Sun[1], Suqi Deng[1], Yingying Wu[1], Xingcheng Liu[1], Caiping Wu[1], Kexiu Huang[1], Yue Li[1], Zexuan Dong[1], Weihao Xiao[1], Manchun Li[2], Zhiyang Chen[2], Zhenyu Ju[2], Jia Xiao[3], Juan Du[1*] and Hui Zeng[4*]

Abstract

Background The function of hematopoietic stem cells (HSC) is regulated by HSC internal signaling pathways and their microenvironment. Chemokines and chemokine ligands play important roles in the regulation of HSC function. Yet, their functions in HSC are not fully understood.

Methods We established *Cxcr3* and *Cxcl10* knockout mouse models ($Cxcr3^{-/-}$ and $Cxcl10^{-/-}$) to analyze the roles of *Cxcr3* or *Cxcl10* in regulating HSC function. The cell cycle distribution of LT-HSC was assessed via flow cytometry. $Cxcr3^{-/-}$ and $Cxcl10^{-/-}$ stem/progenitor cells showed reduced self-renewal capacity as measured in serial transplantation assays. To study the effects of *Cxcr3* or *Cxcl10* deficient bone marrow microenvironment, we transplanted CD45.1 donor cells into $Cxcr3^{-/-}$or $Cxcl10^{-/-}$ recipient mice (CD45.2) and examined donor-contributed hematopoiesis.

Results Deficiency of *Cxcl10* and its receptor *Cxcr3* led to decreased BM cellularity in mice, with a significantly increased proportion of LT-HSC. $Cxcl10^{-/-}$ stem/progenitor cells showed reduced self-renewal capacity in the secondary transplantation assay. Notably, $Cxcl10^{-/-}$ donor-derived cells preferentially differentiated into B lymphocytes, with skewed myeloid differentiation ability. Meanwhile, *Cxcr3*-deficient HSCs demonstrated a reconstitution disadvantage in secondary transplantation, but the lineage bias was not significant. Interestingly, the absence of *Cxcl10* or *Cxcr3* in bone marrow microenvironment did not affect HSC function.

Conclusions The *Cxcl10* and *Cxcr3* regulate the function of HSC, including self-renewal and differentiation, adding to the understanding of the roles of chemokines in the regulation of HSC function.

Keywords C-X-C motif chemokine receptor 3, C-X-C motif chemokine ligand 10, Hematopoietic stem cells, Self-renewal, Competitive bone marrow transplantation

*Correspondence:
Juan Du
du.juan@u.nus.edu
Hui Zeng
androps2011@hotmail.com
[1]Department of Hematology, The First Affiliated Hospital of Jinan University, 613W Huangpu Rd, Guangzhou, Guangdong 510632, China
[2]Key Laboratory of Regenerative Medicine of Ministry of Education, Institute of Aging and Regenerative Medicine, College of Life Science and Technology, Jinan University, Guangzhou, Guangdong 510632, China
[3]Clinical Medicine Research Institute, the First Affiliated Hospital of Jinan University, Guangzhou 510632, China
[4]Department of Hematology, Guangdong Provincial People's Hospital (Guangdong Academy of Medical Sciences), Southern Medical University, 106 Zhongshan 2nd Rd, Guangzhou, Guangdong 510000, China

Introduction

Hematopoietic stem cells (HSC) are a group of adult stem cells with multilineage differentiation and self-renewal capability. The balanced state between quiescence, proliferation, and differentiation is regulated by numerous transcriptional networks, which are controlled by both cellular autonomous factors and the surrounding BM microenvironment [1–3]. Non-hematopoietic cells in the bone marrow niche, such as vascular endothelial cells, adipocytes, and mesenchymal stem cells, have also been identified as key regulators of HSC maintenance [2].

Chemokines belong to the largest subfamily of cytokines and can be further divided into four main subfamilies based on the location of the N-terminal cysteine residues: CC, CXC, XC, and CX3C chemokines [4]. Chemokines normally bind to chemokine receptors, which are widely involved in cell migration, immune cell development and hematopoiesis [5, 6]. HSC proliferation, survival, and differentiation are regulated by members of the chemokine and chemokine receptor family [6]. For example, CXCL12 and its receptor CXCR4 play important roles in hematopoietic cell survival, bone marrow retention, and mobilization [7]. Plerixafor is a CXCR4 antagonist that has been used clinically to mobilize HSCs [8, 9]. Moreover, bone marrow dendritic cells play an important role in regulating hematopoietic stem and progenitor cell (HSPC) trafficking through regulating sinusoidal endothelial cells CXCR2-CXCL1/CXCL2 signaling and vascular permeability [10]. Recent advances have shown that G protein-coupled receptor 182 (GPR182) is expressed in endothelial cells and binds to CXCL10, CXCL12, and CXCL13. GPR182 is a novel atypical chemokine receptor involved in regulating HSC homeostasis through clearance of CXCL10, CXCL12 and CXCL13 [11]. Moreover, studies in Cxcl4-deficient mice showed significantly reduced numbers of HSCs. In contrast, Cxcr2 deficient mice significantly increased the numbers of HSCs and hematopoietic progenitor cell subpopulations. In serial transplantation assays, CXCL4 or CXCR2 deficient HSCs demonstrated significantly reduced self-renewal capacity [12]. However, the roles of chemokines and their receptors in the fate of HSCs have not been comprehensively described so far.

Studies have shown that C-X-C motif chemokine ligand 10 (CXCL10) expression is significantly increased in quiescent hematopoietic stem cells ($CD34^+CD38^-$) compared with proliferative hematopoietic stem progenitor cells ($CD34^+CD38^+$) [12, 13], suggesting that CXCL10 may be involved in regulating HSC homeostasis. C-X-C motif chemokine receptor 3 receptor 3 (CXCR3), as a receptor for CXCL9/CXCL10/CXCL11, is involved in regulating cell proliferation, migration, and immunity, but its role in HSC remains unknown. Here, we investigated the requirement of *Cxcl10* and *Cxcr3* for the self-renewal and multi-lineage differentiation potential of HSCs in vivo.

Methods

Mice

The *Cxcr3*$^{-/-}$ and *Cxcl10*$^{-/-}$ mice were purchased from the Shanghai Model Organism Center. The frameshift mutations were generated by non-homologous recombination using CRISPR-CAS9 technology on the C57BL/6J mouse background. Heterozygous mice were crossed to produce *Cxcl10* or *Cxcr3* deletion homozygous mice. CD45.1 mice were a gift from Dr. Jinyong Wang (Guangzhou Institutes of Biomedicine and Health, Chinese Academy of Sciences, Guangzhou). 8–10 weeks old and sex matched WT and *Cxcr3*$^{-/-}$ or *Cxcl10*$^{-/-}$ mice were used in our study. The mice had access to sterilized food and water ad libitum. Mice were anesthetized with 2% isoflurane and then sacrificed by cervical dislocation. All animal experiments were carried out using the experimental scheme approved by the Institutional Animal Care and Use Committee of Jinan University (JNU-IACUC). All animal experiments were performed according to the National Institutes of Health guide for the care and use of laboratory animals and ARRIVE guidelines. To prevent confounding bias, the placement of each mouse cage was randomized.

Cell staining for FACS analysis and sorting

Bone marrow cells were obtained from the tibia and femur of mice. A small amount of peripheral blood was collected from the retroorbital venous plexus after anesthesia. Spleen cells were obtained by grinding and filtering the spleen. Red blood cells were lysed for subsequent staining. HSPC populations were stained with the following antibodies: LT-HSC ($Lin^-Sca\text{-}1^+c\text{-}Kit^+CD135^-CD150^+CD48^-$); ST-HSC ($Lin^-Sca\text{-}1^+c\text{-}Kit^+CD135^-CD150^-CD48^-$); MPP2($Lin^-Sca\text{-}1^+c\text{-}Kit^+CD135^-CD150^+CD48^+$); MPP3 ($Lin^-Sca\text{-}1^+c\text{-}Kit^+CD135^-CD150^-CD48^+$); MPP4 ($Lin^-Sca\text{-}1^+c\text{-}Kit^+CD135^+CD150^-$ $CD48^+$). For lineage analysis, cells were stained with antibodies against T cells (CD90.2 or CD3), B cells (CD19) and myeloid cells (CD11b). Cell analysis was performed with FACS Canto and FACS Aria III, respectively. Data analysis was performed with FlowJo software.

LT-HSC cell cycle analysis

BM cells were harvested from tibias and femurs of 8-10-week-old WT and *Cxcl10*$^{-/-}$ or *Cxcr3*$^{-/-}$. We first labeled the LT-HSC ($Lin^-Sca\text{-}1^+c\text{-}Kit^+CD135^-CD150^+CD48^-$). Then the cells were fixed using 4% PFA. After washing, the fixed cells were permeabilized with 0.4% saponin in PBS (S4521, Sigma-Aldrich) together with the Ki-67-APC (Cat: 652405,

Biolegend) staining for 45 min. Finally, the cells were resuspended in DAPI solution (2.5 μg/ml) for 1 h in the dark. The data were analyzed using Flowjo software. To prevent confounding bias, the placement of each mouse cage was randomized.

Bone marrow transplantation assays

In non-competitive transplantation experiments, 1×10^6 BM cells from CD45.1 mouse were transplanted into lethally irradiated (8 Gy, 1 Gy/min) *Cxcr3*$^{-/-}$ or *Cxcl10*$^{-/-}$ recipient by the tail vein injection. In competitive transplantation experiments, 5×10^5 *Cxcr3*$^{-/-}$ or *Cxcl10*$^{-/-}$ BM cells were respectively mixed with the same amount of CD45.1 BM cells and transferred into lethally irradiated (8 Gy, 1 Gy/min) CD45.1 recipients by the tail vein injection. The second transplantation was performed *at* 16 weeks. 1×10^6 BM cells from primary recipients were injected into lethally irradiated (8 Gy, 1 Gy/min) CD45.1 recipients by tail vein injection. Donor chimerism and lineage commitment of peripheral blood were assessed every 4 weeks by flow cytometric analysis. At the end of transplantation, recipients were sacrificed and BM HSPC frequency was determined. To prevent confounding bias, the placement of each mouse cage was randomized.

RNA-seq of LT-HSCs and analysis

LT-HSCs ($Lin^-Sca\text{-}1^+c\text{-}Kit^+CD135^-CD150^+CD48^-$) were isolated from bone marrow cells of three WT mice, *Cxcl10*$^{-/-}$ and *Cxcr3*$^{-/-}$ mice, respectively. 500 ~ 800 drops per mouse were sorted into 96-well plates containing 10 μl buffer (2%FBS + DPBS). RNA extraction and amplification were performed with Discover-sc WTA Kit V2 following the manufacturer's instructions (Vazyme, N711-02). cDNA concentration was determined by Qubit 3.0. Sequencing libraries were prepared using TruePrep DNA Library Prep Kit V2 for Illumina according to the manufacturer's protocol (Vazyme, TD503-01) and sequenced on the Illumina sequencing platform by Genedenovo Biotechnology Co., Ltd (Guangzhou, China). Alignment analysis of mouse genomes was carried out using HISAT2 software [14]. RSEM was used to calculate the expression of all genes in each sample [15]. Differential gene expression analysis was performed by the DESeq2 package. GSEA analysis was used to find enriched signaling pathways.

Statistical analysis

The data were represented as mean values ± SD or SEM and analyzed using GraphPad Prism software (Version 8.0). Two-tailed Student's t-tests were performed for the comparison of two groups. *P* values of less than 0.05 were considered statistically significant (*:$P<0.05$, **:$P<0.01$, ***:$P<0.001$, ****: $P<0.0001$).

ARRIVE checklist

All authors declare that the work has been reported in line with the ARRIVE guidelines 2.0.

Results

Loss of *Cxcl10* increased proportion of LT-HSC under homeostasis

To study the role of *Cxcl10* in hematopoiesis, *Cxcl10*$^{-/-}$ mice were established with CRISPR/Cas9 method (Fig. S1A). The deletion of *Cxcl10* was confirmed by polymerase chain reaction (PCR) (Fig. S1B). In 8-10-week-old, weight-and sex-matched mice, the number of bone marrow cells significantly decreased in *Cxcl10*$^{-/-}$ mice compared to WT mice ($P<0.001$) (Fig. 1A, Fig. S2A). Interestingly, both the weight and cell counts of the spleen increased in *Cxcl10*$^{-/-}$ mice ($P<0.001$) (Fig. 1B-C). We next examined the frequencies of mature lineages in the peripheral blood, bone marrow, and spleen. The frequencies of lineage cells ($CD90.2^+$ T cells, $CD19^+$ B cells, and $CD11b^+$ myeloid cells) were comparable to those in WT mice (Fig. 1D-E). However, the frequency of T cells decreased and that of B cells increased in the spleen of *Cxcl10*$^{-/-}$ mice ($P<0.001$) (Fig. 1F). We then went on to examine the T cell distribution in the thymus and found no significant difference in the proportion of T lymphocyte subsets in the thymus of *Cxcl10*$^{-/-}$ mice (Fig. S2B). Next, we investigate whether the deficiency of Cxcl10 affects HSPCs. Interestingly, we observed an increase in the proportion of LT-HSC, ST-HSC, MPP4 as well as the LSK in the bone marrow of *Cxcl10*$^{-/-}$ mice (Fig. 1G-I). To further characterize the *Cxcl10*$^{-/-}$ HSCs, we examined the cell cycle status of *Cxcl10*$^{-/-}$ LT-HSC. Notably, the ratio of *Cxcl10*$^{-/-}$ in the G0 phase was reduced significantly while more *Cxcl10*$^{-/-}$ LT-HSCs were in the G1-S-G2-M phase compared to WT mice ($P<0.05$), indicating loss of Cxcl10 drives HSCs into cell cycle (Fig. 1J-L). Taken together, *Cxcl10* deficiency alters the cellularity in the bone marrow and spleen. More importantly, the loss of *Cxcl10* increases the frequency of LT-HSCs and drives them into the cell cycle.

Loss of *Cxcr3* increased proportion of LT-HSC under homeostasis

To complement the observation in *Cxcl10*$^{-/-}$ mice, we next investigated the requirement of *Cxcr3*, a receptor for *Cxcl10*, for HSC function in mice. Similarly, *Cxcr3*$^{-/-}$ mice were constructed with CRISPR9/Cas9 method and confirmed by PCR (Fig. S3). In 8-10-week-old, weight- and sex-matched mice, the number of bone marrow cellularity significantly decreased ($P<0.01$) (Fig. 2A, Fig. S4A), while the weight and cell counts of spleen also increased in *Cxcr3*$^{-/-}$ mice (Fig. 2B-C). The frequency of mature lineage cells ($CD90.2\ T^+$ cells, $CD19^+$ B cells, and $CD11b^+$ myeloid cells) in *Cxcr3*$^{-/-}$ mice in peripheral

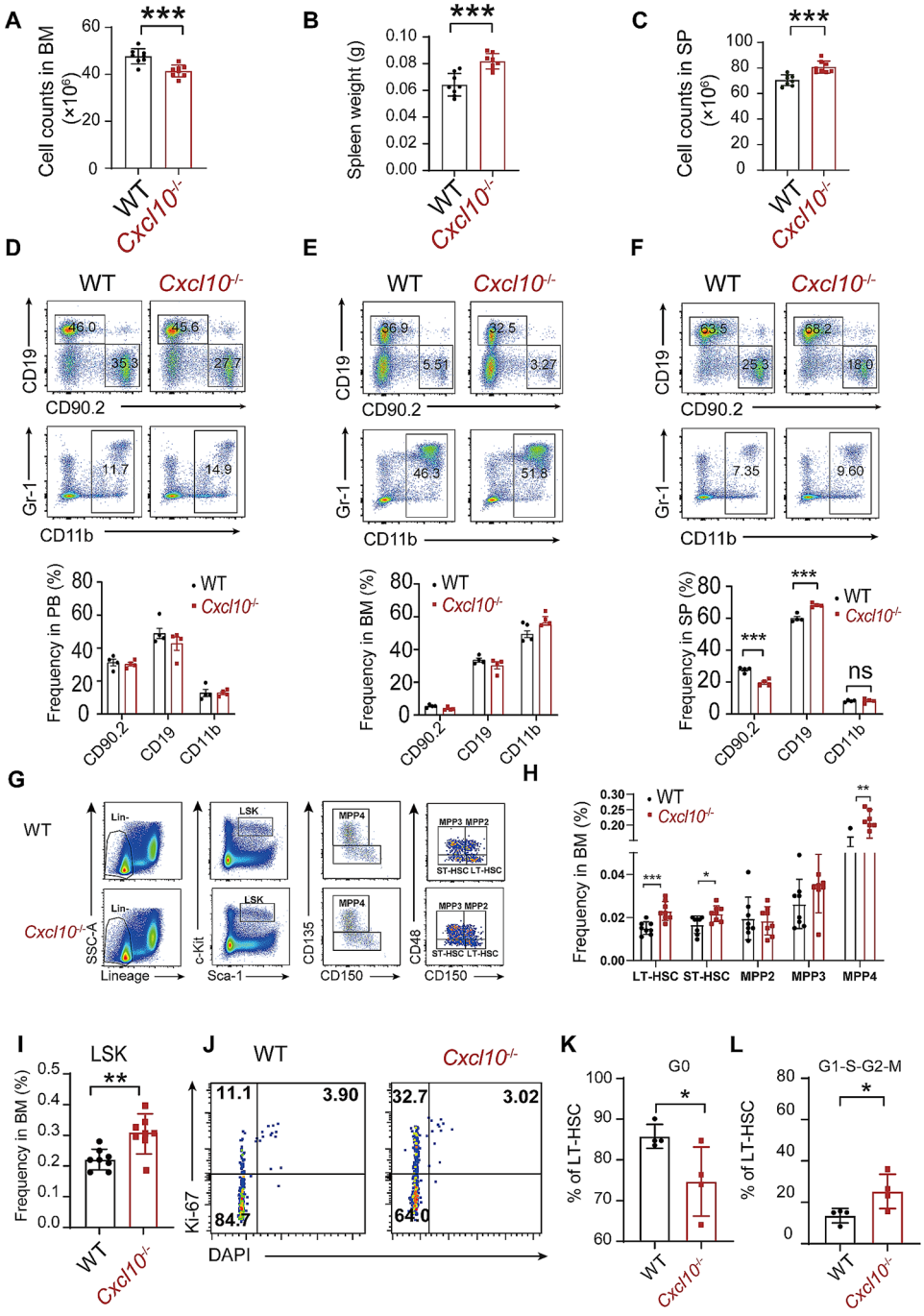

Fig. 1 The HSPC and lineage composition of *Cxcl10*$^{-/-}$ mice under homeostasis. (**A**-**C**) Counts of bone marrow cells (**A**), weight of spleen (**B**), number of spleen cells (**C**) in *Cxcl10*$^{-/-}$ mice. Data are analyzed by Student's t-test ($n=8$ mice for each group, a total of 16). ***, $P<0.001$. (**D**-**F**) The proportion of T lymphocytes, B lymphocytes, and myeloid cells from PB (**D**), BM (**E**), and SP (**F**) in *Cxcl10*$^{-/-}$ mice. Data are analyzed by Student's t-test ($n=4$ mice for each group, a total of 8). ***, $P<0.001$. (**G**-**I**) (**G**) Representative gating strategy used to identify LT-HSC, ST-HSC, MPP2, MPP3, and MPP4 based on expression of CD135, CD48, and CD150 in BM LSK in *Cxcl10*$^{-/-}$. (**H**) Statistical analysis of HSPC proportion in *Cxcl10*$^{-/-}$ mice. (**I**) Statistical analysis of LSK proportion in *Cxcl10*$^{-/-}$ mice. Data are analyzed by Student's t-test ($n=8$ mice for each group, a total of 16). *, $P<0.05$, **, $P<0.01$, ***, $P<0.001$. (**J**-**L**) Cell cycle analysis of *Cxcl10*$^{-/-}$ HSCs under homeostasis. (**J**) Representative plots of cell cycle from representative WT and *Cxcl10*$^{-/-}$ mice (6-week-old). WT littermates (6-week-olds) were used as control. LT-HSC (Lin^- ($CD2^-$ $CD3^-$ $CD4^-$ $CD8^-$ $B220^-$ $Gr1^-$ $CD11b^-$ $Ter119^-$) $CD48^-$ $Sca1^+$ $c\text{-}kit^+$ $CD150^+$ $CD135^-$) were analyzed by DNA content (DAPI) versus Ki-67. G0 ($Ki\text{-}67^-DAPI^-$), G1-G2-S-M ($Ki\text{-}67^+$). The percentages (%) of LT-HSC in G0 (**K**), G1-G2-S-M (**L**) stages were compared, respectively. Data are analyzed by Student's t-test ($n=4$ mice for each group, a total of 8). *, $P<0.05$

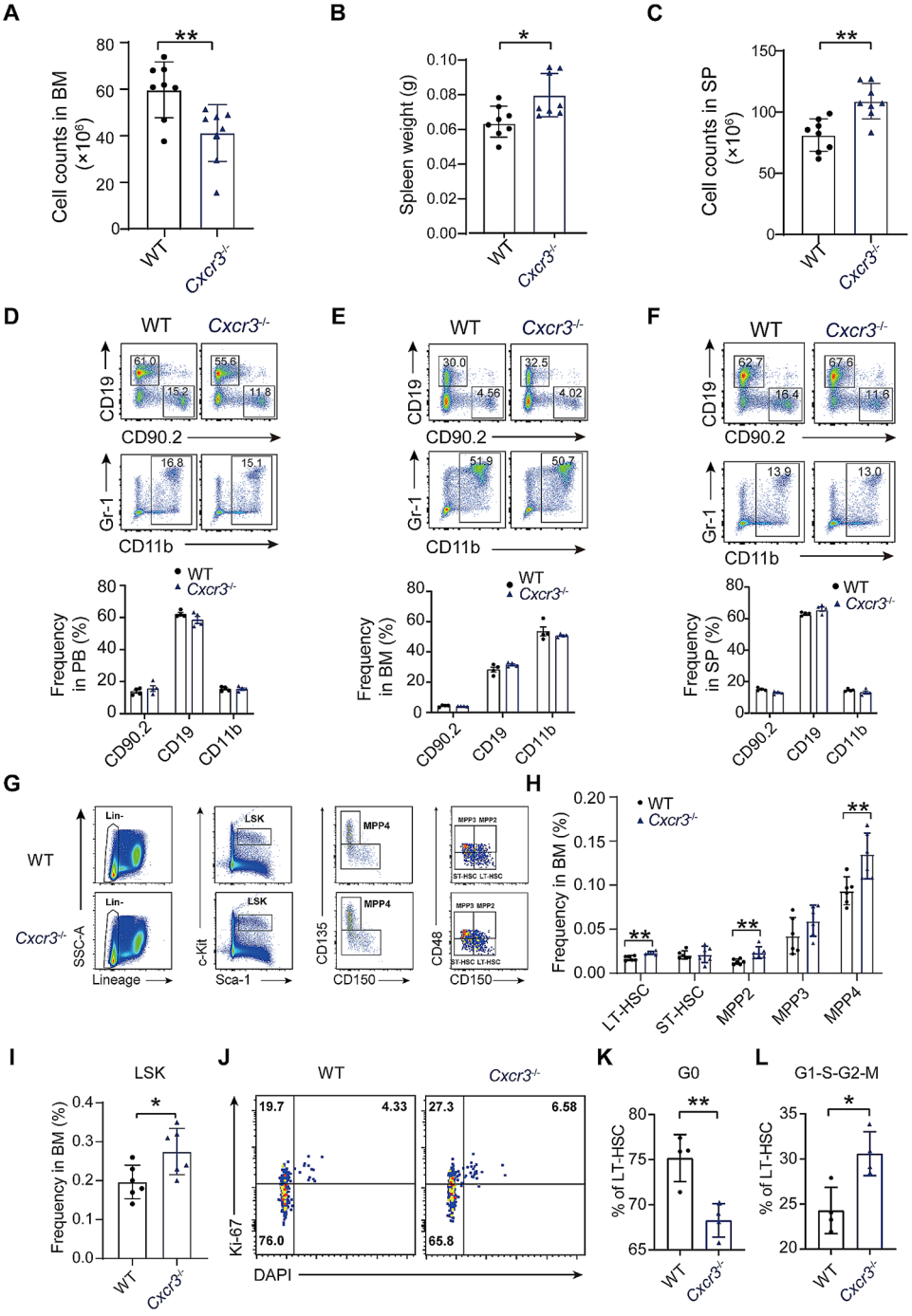

Fig. 2 The HSPC and lineage composition of *Cxcr3*$^{-/-}$ mice under homeostasis.(**A**-**C**) Counts of bone marrow cells (**A**), weight of spleen (**B**), number of spleen cells (**C**) in *Cxcr3*$^{-/-}$ mice. Data are analyzed by Student's t-test ($n=8$ mice for each group, a total of 16). *, $P<0.05$, **, $P<0.01$. (**D**-**F**) The proportion of T lymphocytes, B lymphocytes, and myeloid cells from PB (**D**), BM (**E**), and SP (**F**) in *Cxcr3*$^{-/-}$ mice ($n=4$ mice for each group, a total of 8). (**G**-**I**) (**G**) Representative gating strategy used to identify LT-HSC, ST-HSC, MPP2, MPP3, and MPP4 based on expression of CD135, CD48, and CD150 in BM LSK in *Cxcr3*$^{-/-}$ mice. (**H**)Statistical analysis of HSPC proportion in *Cxcr3*$^{-/-}$ mice. (**I**) Statistical analysis of LSK proportion in *Cxcr3*$^{-/-}$ mice. Data are analyzed by Student's t-test ($n=6$ mice for each group, a total of 12). *, $P<0.05$. (**J**-**K**) Cell cycle analysis of *Cxcr3*$^{-/-}$ HSCs under homeostasis. (**J**) Representative plots of cell cycle from representative WT and *Cxcr3*$^{-/-}$ mice (6-week-old). WT littermates (6-week-olds) were used as controls. LT-HSC (Lin$^-$ (CD2$^-$ CD3$^-$ CD4$^-$ CD8$^-$ B220$^-$ Gr1$^-$ CD11b$^-$ Ter119$^-$) CD48$^-$ Sca1$^+$ c-kit$^+$ CD150$^+$ CD135$^-$) were analyzed by DNA content (DAPI) versus Ki-67. G0 (Ki-67$^-$DAPI$^-$), G1-G2-S-M (Ki-67$^+$). The percentages (%) of LT-HSC in G0 (**K**), G1-G2-S-M (**L**) stages were compared, respectively. Data are analyzed by Student's t-test ($n=4$ mice for each group, a total of 8). *, $P<0.05$, **, $P<0.01$

blood, BM, and spleen were all comparable to WT mice (Fig. 2D-F). Not surprisingly, no differences were detected in the T-cell subsets (CD4 and CD8) in the thymus between the *Cxcr3*$^{-/-}$ mice and WT mice (Fig. S4B). Next, we also investigate whether the deficiency of Cxcr3 affects HSPCs. We observed an increase in the proportion of LT-HSC, MPP2, MPP4, and LSK in the bone marrow of *Cxcr3*$^{-/-}$ mice (Fig. 2G-I). The cell cycle analysis of LT-HSC indicated that fewer LT-HSCs were in G0 status while more cells entered the G1-S-G2-M phase (Fig. 2J-L). Collectively, *Cxcr3* deficiency leads to the alteration of cellularity in the bone marrow and spleen, and loss of *Cxcr3* also results in the increase of phenotypic LT-HSCs and drives them into the cell cycle.

Cxcl10 or *Cxcr3* deficient HSCs showed normal reconstitution capacity in primary transplantation

To further investigate the role of *Cxcl10* and *Cxcr3* in the function of HSCs, we performed a competitive transplantation assay. Five hundred thousand whole bone marrow cells from *Cxcl10*$^{-/-}$ or *Cxcr3*$^{-/-}$ (CD45.2^{+}) were transplanted into irradiated recipients (CD45.1^{+}) respectively, together with five hundred thousand CD45.1^{+} competitor cells (Fig. 3A). Donor chimerism and lineage composition of the peripheral blood were assessed by flow cytometry every four weeks. The donor contribution of *Cxcl10*$^{-/-}$ or *Cxcr3*$^{-/-}$ mice in PB was comparable with WT control in primary recipients (Fig. 3B-C). Consistently, we found no alteration in percentages of T lymphocytes, B lymphocytes, and myeloid cells in donor-derived cells (Fig. 3D-F, Fig. S5). When compared with the WT control, we also observed comparable percentages of LSK and LT-HSC in the donor-derived cells in the recipient mice for both Cxcl10 and Cxcr3 groups (Fig. 3G-H). These data suggest that *Cxcl10* and *Cxcr3* deficient HSCs have normal reconstitution capacity in the primary transplantation recipients.

Cxcl10 and *Cxcr3* deficiency decreases self-renewal of HSCs in secondary recipient mice

Since we found the loss of *Cxcl10* and *Cxcr3* induced cell cycle entry of HSC in the primary mice, we speculate that the loss of *Cxcl10* and *Cxcr3* might lead to self-renewal defect of these HSCs in more stressed conditions. To determine the effect of *Cxcl10* and *Cxcr3* in long-term engraftment, we performed secondary transplantation by transplanting one million total bone marrow cells of the primary recipients into lethally irradiated recipients (CD45.1). Intriguingly, there was a significant decrease of donor contribution in the peripheral blood of recipients transplanted with *Cxcl10*$^{-/-}$ cells 4 weeks post-transplantation, while a significant decrease of donor contribution became prominent for *Cxcr3*$^{-/-}$ 8 weeks post-transplantation (Fig. 4A-B). Interestingly, we observed that the percentage of B cells increased significantly, while the percentage of myeloid cells decreased markedly in the PB of *Cxcl10*$^{-/-}$ secondary recipient mice. However, there was no obvious bias in the lineage differentiation of the *Cxcr3*$^{-/-}$ group up to 16 weeks post-transplantation (Fig. 4C-E, Fig. S6). Sixteen weeks after transplantation, we sacrificed the secondary recipients and analyzed the lineage distribution in the spleen. The donor contribution in the spleen dropped dramatically for both *Cxcl10*$^{-/-}$ and *Cxcr3*$^{-/-}$ groups. Notably, donor contribution of myeloid cells deceased for the *Cxcl10*$^{-/-}$ recipients, while the percentage of B cells increased compared to the WT control group (Fig. 4F-G). Within the LSK and LT-HSC compartments, the donor-contribution of the *Cxcl10*$^{-/-}$ group also decreased significantly compared to the WT or *Cxcr3*$^{-/-}$ group (Fig. 4H-I). The above data indicates that both loss of *Cxcl10* and its receptor *Cxcr3* affect the long-term reconstitution capacity of HSC while *Cxcl10* plays a role in determining myeloid and B lineages.

Lack of *Cxcl10* or *Cxcr3* drives HSCs into the cell cycle upon irradiation exposure

Since we observed the reconstitution disadvantage of *Cxcl10*$^{-/-}$ and *Cxcr3*$^{-/-}$ HSCs in the transplantation setting, we wonder whether deficiency of *Cxcl10* and *Cxcr3* could alter HSC function in other stress conditions. To address this question, we irradiated these mice in parallel with WT control mice at 4 Gy and examined the frequencies and cell cycle of the HSPC compartment 6 h after exposure (Fig. 5A). The ratio of *Cxcl10*$^{-/-}$ in G0-status was reduced significantly, as more *Cxcl10*$^{-/-}$ LT-HSCs entered the G1-S-G2 and M phase as expected (**, $P<0.01$, ***, $P<0.001$) (Fig. 5B-D), indicating an accelerated cell cycle entry in response to irradiation. Similarly, the proportion of quiescent cells in the *Cxcr3*$^{-/-}$ HSC also decreased and an increase of cycling cells (G1-S-G2-M proliferative phases) in the residual *Cxcr3*$^{-/-}$ HSC was observed ($P<0.01$) (Fig. 5E-G). Therefore, *Cxcr3*$^{-/-}$ and *Cxcl10*$^{-/-}$ HSCs were more susceptible to irradiation-induced stress, and the residual HSCs proliferated shortly after irradiation, leading to a rapid increase of phenotypic HSCs.

Lack of *Cxcl10* or *Cxcr3* in bone marrow microenvironment did not affect HSC function

Our data suggest that *Cxcl10* and *Cxcr3* regulate HSC in a cell-autonomous manner. To exclude a non-cell-autonomous role of *Cxcl10*, we performed retrospective transplantation by transplanting CD45.1 bone marrow cells into irradiated *Cxcl10*$^{-/-}$ recipients (Fig. 6A). Interestingly, the absence of *Cxcl10* from the niche components failed to demonstrate obvious defect to support normal reconstitution of CD45.1 HSCs (Fig. 6B-E). Similarly, retrospective transplantation of *Cxcr3* was performed

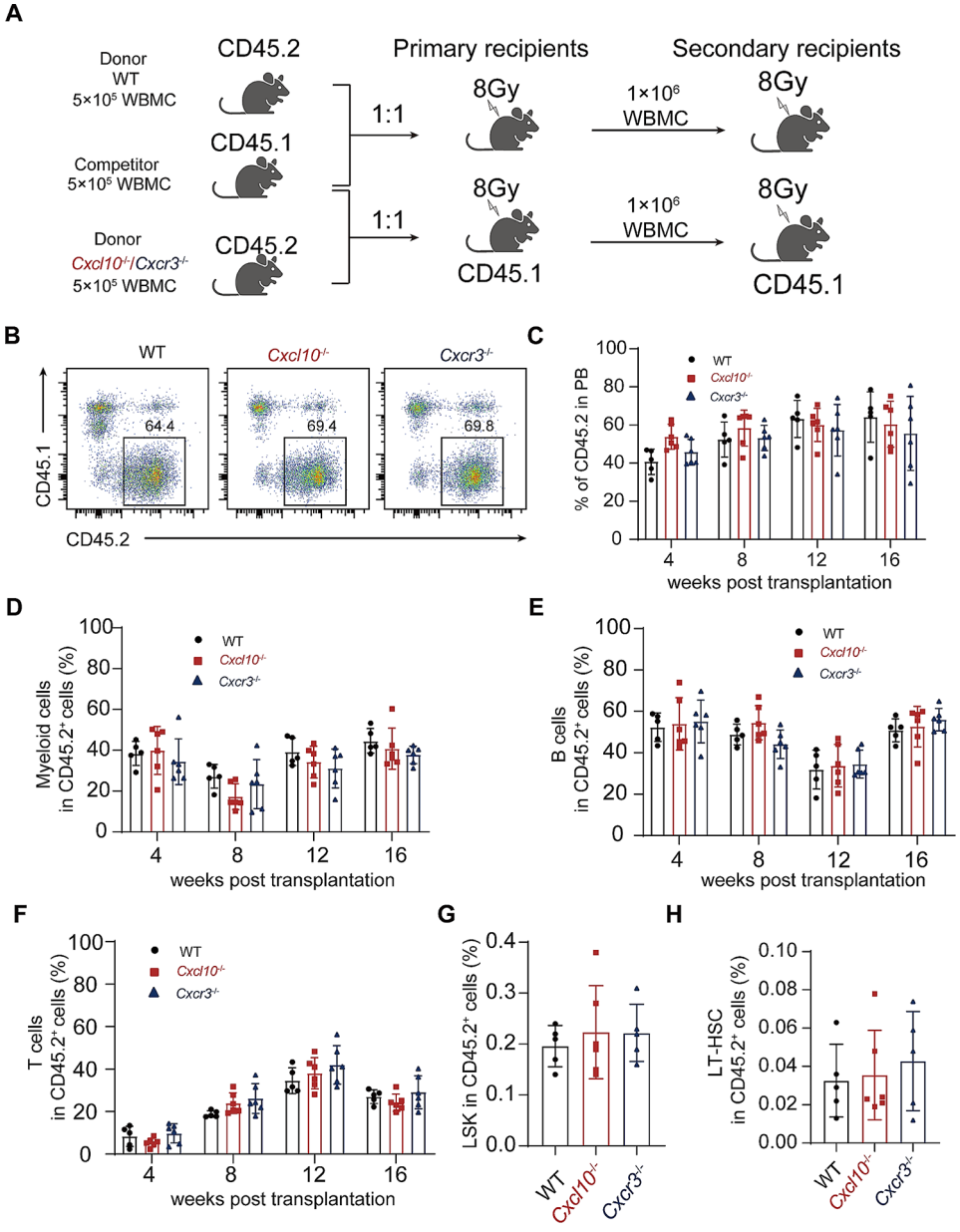

Fig. 3 *Cxcl10*$^{-/-}$/*Cxcr3*$^{-/-}$ HSCs show no difference in engraftment in primary transplantation assays. (**A**) Schematic diagram of competitive transplantation assay. 5×10^5 donor *Cxcl10*$^{-/-}$ / *Cxcr3*$^{-/-}$ WBMC (CD45.2) or littermate control WBMC (CD45.2) were mixed with equivalent WT (CD45.1) counterparts and transplanted to lethally irradiated recipients (CD45.1). 16 weeks later, the primary recipients were sacrificed. 1×10^6 WBMC were transplanted to lethally irradiated secondary recipients (CD45.1). (**B**) Representative flow cytometry plots of donor chimerism of primary transplanted recipients. (**C**) Donor population was analyzed in the peripheral blood from primary recipients ($n = 5$ mice for WT, $n = 6$ mice for *Cxcl10*$^{-/-}$, $n = 6$ mice for *Cxcr3*$^{-/-}$, a total of 17). (**D**-**F**) Donor-derived lineage chimerism in PB from primary transplanted recipients, including myeloid cells (**D**), B lymphocytes (**E**), and T lymphocytes (**F**) ($n = 5$ mice for WT, $n = 6$ mice for *Cxcl10*$^{-/-}$, $n = 6$ mice for *Cxcr3*$^{-/-}$, a total of 17). (**G**-**H**). Statistical analysis of LSK and LT-HSC proportion of CD45.2 in WT mice, *Cxcl10*$^{-/-}$ mice and *Cxcr3*$^{-/-}$ mice ($n = 5$ mice for WT, $n = 6$ mice for *Cxcl10*$^{-/-}$, $n = 5$ mice for *Cxcr3*$^{-/-}$, a total of 16)

to investigate whether loss of *Cxcr3* from the niche cells could lead to defects of residing HSC (Fig. 6F). To our surprise, although the contribution of donor cells was decreased in the peripheral blood and T cells for week 8 and week 16, we failed to observe severe defect to support normal hematopoiesis of CD45.1 HSC (Fig. 6G-J). These data indicated that the lack of *Cxcl10* or *Cxcr3* in the bone marrow microenvironment did not affect HSC function in a non-cell-autonomous manner.

Potential mechanism of *Cxcl10* and *Cxcr3* in regulating HSC functions

To gain insights into the possible mechanism by which *Cxcl10* and *Cxcr3* deletion impairs the self-renewal of

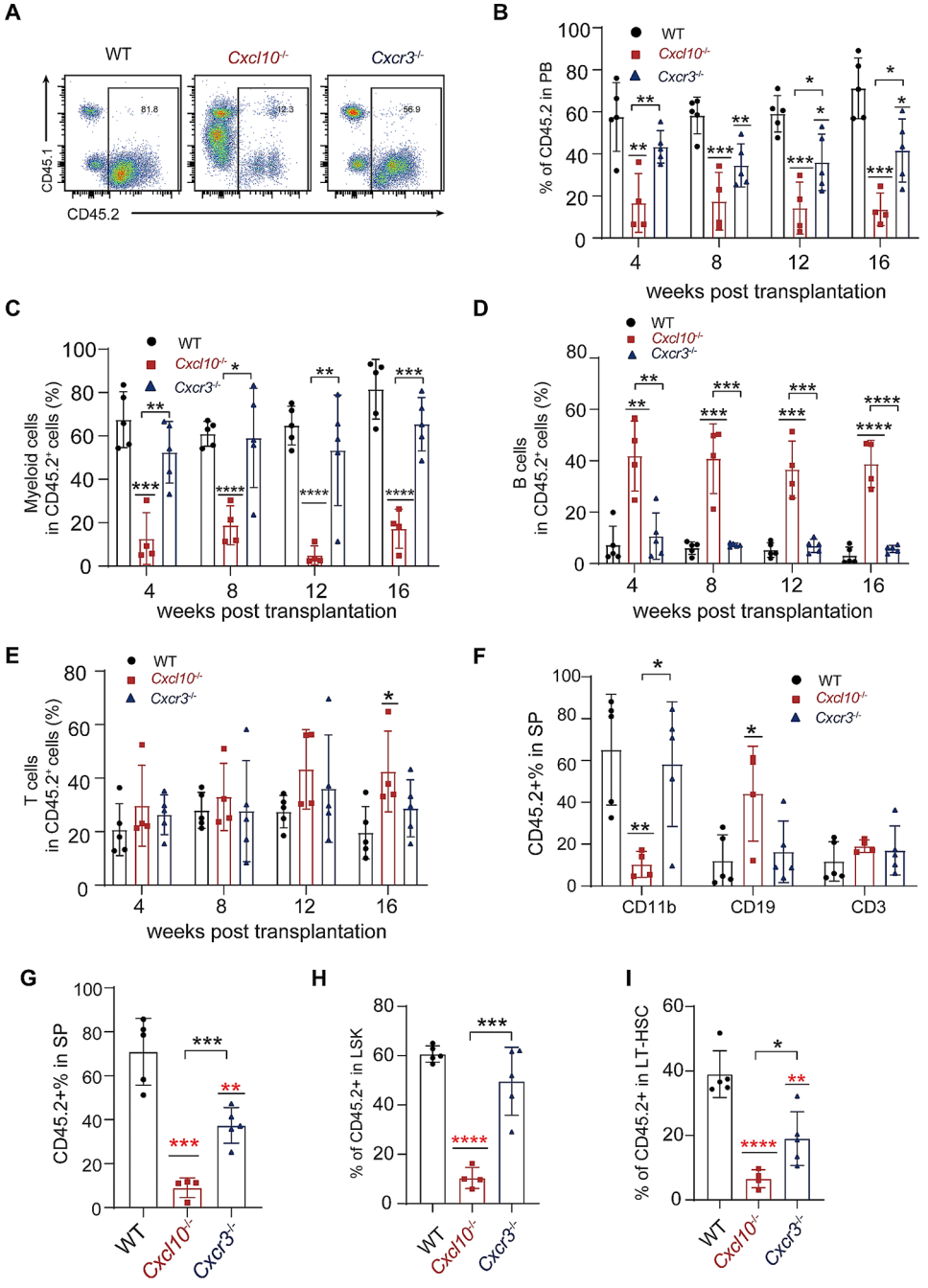

Fig. 4 *Cxcl10*$^{-/-}$/*Cxcr3*$^{-/-}$ HSCs show a reduction in engraftment in secondary transplantation assays. (**A**) Representative flow cytometry plots of donor chimerism of secondary transplanted recipients. (**B**) Donor population was analyzed in the peripheral blood from secondary recipients Data are analyzed by Student's t-test ($n=5$ mice for WT, $n=4$ mice for *Cxcl10*$^{-/-}$, $n=5$ mice for *Cxcr3*$^{-/-}$, a total of 14). *, $P<0.05$, **, $P<0.01$, ***, $P<0.001$. (**C**-**E**) Donor-derived lineage chimerism in PB from secondary transplanted recipients, including myeloid cells (**C**), B lymphocytes (**D**), and T lymphocytes (**E**). Data are analyzed by Student's t-test ($n=5$ mice for WT, $n=4$ mice for *Cxcl10*$^{-/-}$, $n=5$ mice for *Cxcr3*$^{-/-}$, a total of 14). *, $P<0.05$, **, $P<0.01$, ***, $P<0.001$, ****, $P<0.0001$. (**F**) Donor-derived lineage chimerism in spleen from secondary transplanted recipients, including myeloid cells, B lymphocytes, and T lymphocytes Data are analyzed by Student's t-test ($n=5$ mice for WT, $n=4$ mice for *Cxcl10*$^{-/-}$, $n=5$ mice for *Cxcr3*$^{-/-}$, a total of 14). *, $P<0.05$, **, $P<0.01$. (**G**) The donor population was analyzed in the spleen from secondary recipients. Data are analyzed by Student's t-test ($n=5$ mice for WT, $n=4$ mice for *Cxcl10*$^{-/-}$, $n=5$ mice for *Cxcr3*$^{-/-}$, a total of 14). **, $P<0.01$, ***, $P<0.001$. (**H**-**I**) Statistical analysis of CD45.2 of LSK and LT-HSC proportion in WT mice, *Cxcl10*$^{-/-}$ mice and *Cxcr3*$^{-/-}$ mice. Data are analyzed by Student's t-test ($n=5$ mice for WT, $n=4$ mice for *Cxcl10*$^{-/-}$, $n=5$ mice for *Cxcr3*$^{-/-}$, a total of 14). *, $P<0.05$, **, $P<0.01$, ***, $P<0.001$, ****, $P<0.0001$

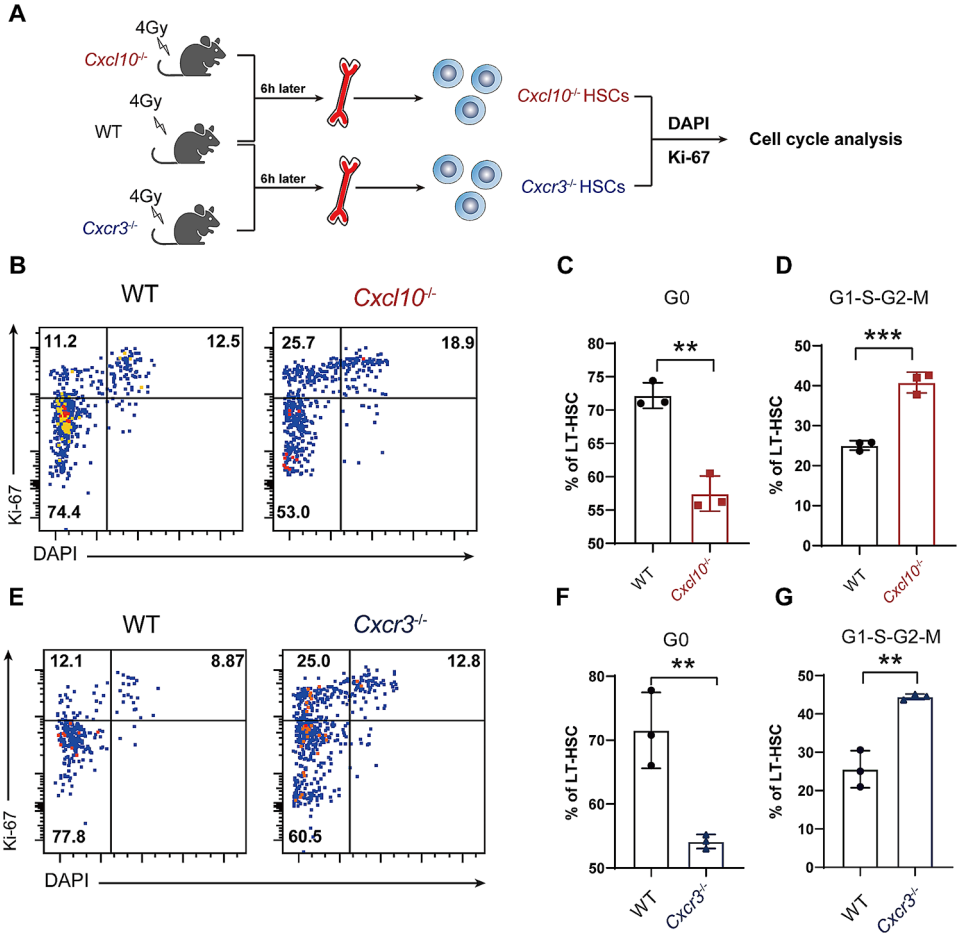

Fig. 5 *Cxcl10*$^{-/-}$/*Cxcr3*$^{-/-}$ HSCs enter into the cell cycle upon irradiation stress. (**A**) Schematic representation of cell cycle analysis of HSCs 6 h after 4 Gy irradiation. (**B**) Representative flow plots of cell cycle analysis of WT (left) and *Cxcl10*$^{-/-}$ (right) mice. (**C**-**D**) Statistical analysis of HSCs in G0 (C, Ki-67^{-} DAPI^{-}) and G1-S-G2-M phase (**D**, Ki-67^{+}) in (**B**), ($n=3$ mice for each group, a total of 6). **, $P<0.01$, ***, $P<0.001$. (**E**) Representative flow plots of cell cycle analysis of WT (left) and *Cxcr3*$^{-/-}$ (right) mice. (**F**-**G**) Statistical analysis of HSCs in G0 (**F**, Ki-67^{-} DAPI^{-}) and G1-S-G2-M (**G**, Ki-67^{+}) phase in (**E**), ($n=3$ mice for each group, a total of 6). **, $P<0.01$

HSCs, we sorted LT-HSCs from *Cxcl10*$^{-/-}$, *Cxcr3*$^{-/-}$ and WT mice for transcriptomic analysis. Differentially-expressed genes (DEGs) were identified based on criteria of adjusted $P<0.05$ and fold change>1.5. A total of 465 DEGs were identified between WT and *Cxcl10*$^{-/-}$ LT-HSC (Fig. 7A) while only 41 DEGs were found for *Cxcr3*$^{-/-}$ HSC compared to control HSCs (Table S1). To further dissect the potential mechanism determining the function of *Cxcl10*$^{-/-}$ LT-HSC, GSEA enrichment analysis were performed (Fig. 7B). Interestingly, GSEA showed that a number of DEGs between the WT and *Cxcl10*$^{-/-}$ LT-HSC DEGs were related to pathways of the G0-early G1 phase and the expression levels of these DEGs were decreased (Fig. 7C-D). These data collectively demonstrate that *Cxcl10* may regulate the quiescence of HSC, the loss of which drives HSCs into the cell cycle.

Discussion

Regulation of hematopoietic stem cell function by chemokines is still largely unknown. Here, we demonstrate that loss of *Cxcl10* increased the phenotypic LT-HSC, ST-HSC, and LSK in the primary mice. More importantly, *Cxcl10* deficient HSCs demonstrated impaired self-renewal and skewed lineage differentiation. While the reconstitution of the primary recipient appeared relatively normal, the donor contribution dropped dramatically for the *Cxcl10* group in the secondary recipients. These data indicated that loss of *Cxcl10* drives HSC into the cell cycle which contributed to the increase of phenotypic HSC in the primary mice but eventually leads to the exhaustion of HSC. Similarly, the loss of *Cxcr3* also impaired the self-renewal of HSC. The donor contribution of mice that received *Cxcr3*-deficient HSC also dropped compared to the control, although to a less severe extent compared to *Cxcl10*. These data suggest that *Cxcl10* and *Cxcr3* play an important role in the

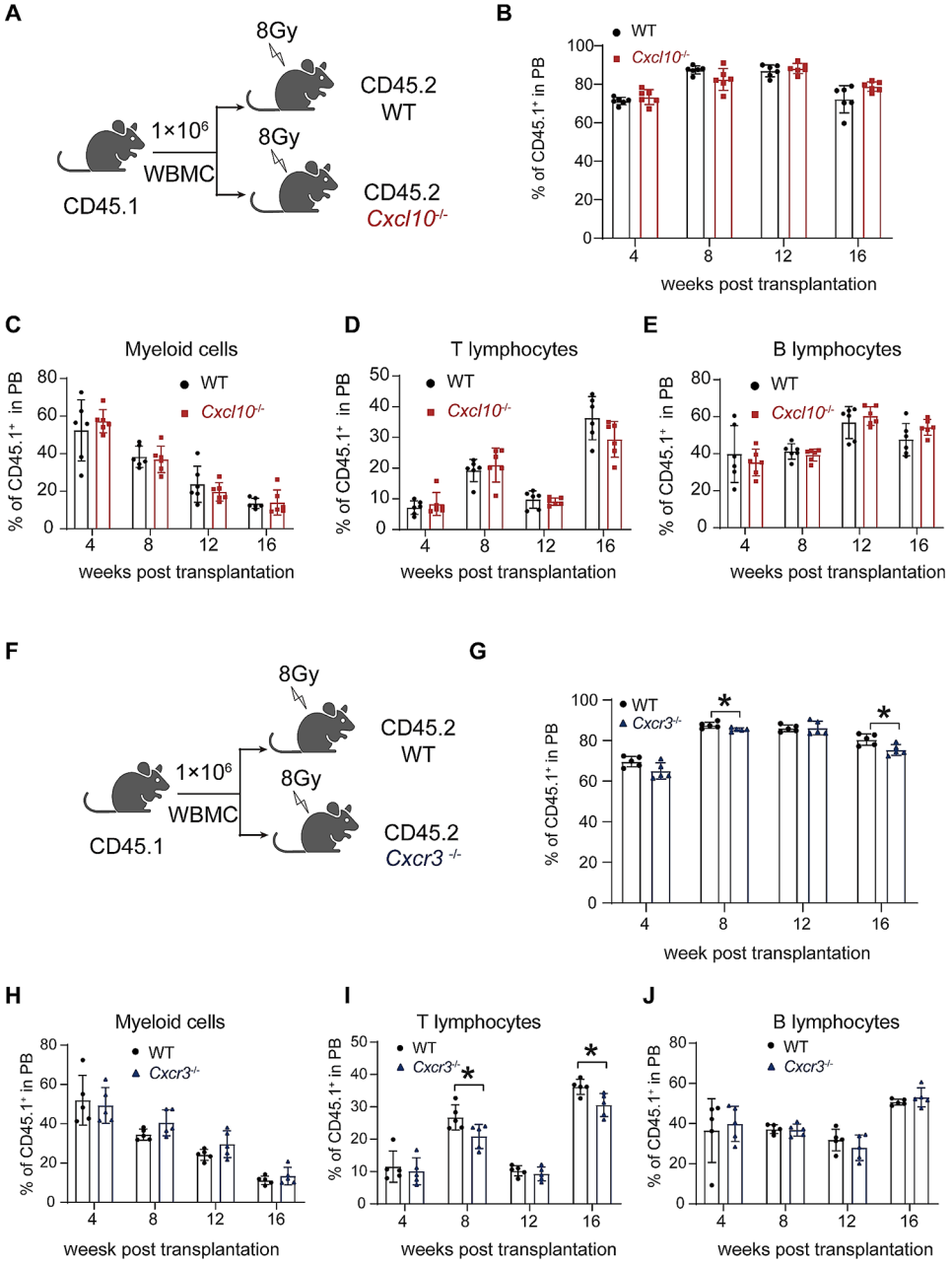

Fig. 6 HSC does not show altered functional differences in the *Cxcl10*- or *Cxcr3*-deficient microenvironment in noncompetitive transplantation. (**A**) Schematic representation of the noncompetitive transplantation strategy. 1×10^6 WT WBMC (CD45.1) were transplanted to lethally irradiated *Cxcl10*$^{-/-}$ (CD45.2) and WT recipient (CD45.2). (**B**) Donor-derived HSPC population from the bone marrow of *Cxcl10*$^{-/-}$ recipients in noncompetitive transplantation at 16 weeks ($n = 6$ mice for each group, a total of 12). (**C**-**E**) Donor-derived lineage chimerism in *Cxcl10*$^{-/-}$ recipients, including myeloid cells, T lymphocytes, and B lymphocytes every 4 weeks post-transplant up to 16 weeks ($n = 6$ mice for each group, a total of 12). (**F**) Schematic representation of the noncompetitive transplantation strategy. 1×10^6 WT WBMC (CD45.1) were transplanted to lethally irradiated *Cxcr3*$^{-/-}$ (CD45.2) and WT recipient (CD45.2). (**G**) Donor-derived HSPC population from the bone marrow of *Cxcr3*$^{-/-}$ recipients in noncompetitive transplantation at 16 weeks ($n = 5$ mice for each group, a total of 10). *, $P < 0.05$. (**H**-**J**) Donor-derived lineage chimerism in *Cxcr3*$^{-/-}$ recipients, including myeloid cells (**H**) T lymphocytes (**I**), and B lymphocytes (**J**) every 4 weeks post-transplant up to 16 weeks ($n = 5$ mice for each group, a total of 10). *, $P < 0.05$

regulation of self-renewal of HSC. Our finding is another piece of data suggesting the role of chemokines in the regulation of self-renewal of HSC. A previous study reported that *Cxcl4* and *Cxcr2* regulate self-renewal and differentiation of HSC with knock-out mice [12]. Of note, the defect of *Cxcl10* and *Cxcr3* knockout HSC could only be observed under stress conditions, including secondary transplantation and irradiation. Whether these HSCs behave similarly in other stress conditions, tertiary

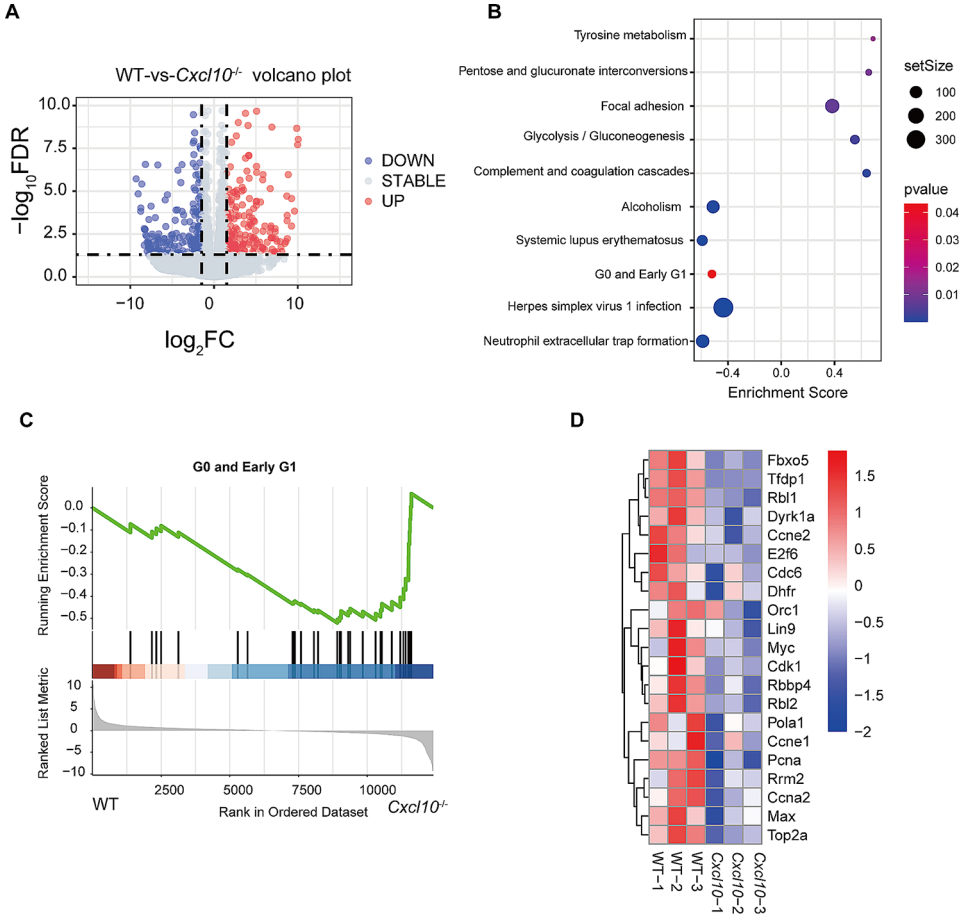

Fig. 7 Gene expression pattern of LT-HSC from *Cxcl10*$^{-/-}$ mice. (**A**) Volcano plot for differentially expressed genes identified in *Cxcl10*$^{-/-}$ and WT LT-HSC. (**B**) Dot plots showing enrichment of KEGG and cell cycle related gene sets in the Cxcl10 knockout LT-HSC, comparing to WT controls. Statistical significance [false discovery rate (FDR)] and a fraction of cells expressing the gene were represented by color and size respectively. (**C**) The gene sets of the G0-early G1 signaling pathway in WT vs. *Cxcl10*$^{-/-}$ from GSEA analysis. (**D**) Heatmap showing the scaled expression level of genes within G0 and early G1 cell cycle pathway in *Cxcl10*$^{-/-}$ and WT LT-HSCs

transplantation or chemotherapy, for example, should be tested in the future.

Interestingly, in addition to the disadvantage of hematopoietic reconstitution in the secondary recipient, we observed lineage bias of *Cxcl10*$^{-/-}$ HSC. Although a significant increase of B cell proportion in the spleen is observed in the primary mice, other hematopoietic lineage seems normal in the *Cxcl10*-deficient mice. However, with two rounds of transplantation, we observed an increase in B cells at the expense of myeloid cells. This is unlikely because of the inability of B cells to mobilize from the spleen to the periphery, as the imbalanced lineage bias is observed both in the spleen and the peripheral blood. While the decreased contribution of donor-derived HSC indicated defect *Cxcl10*$^{-/-}$ HSC, how the loss of *Cxcl10* affects downstream signaling cascades that eventually determine the lineage specification worth further investigation. It would be interesting to know whether the loss of *Cxcl10* contributed to the altered expression or function of the essential transcription factors which may regulate the switch between the myeloid and B lineages.

More importantly, we observed normal hematopoietic reconstitution for retrospective transplantation. Neither loss of *Cxcl10* nor *Cxcr3* induced impaired function of HSC. Combined with the data from competitive transplantation, these results suggest that *Cxcl10* and *Cxcr3* play an important role in regulating the self-renewal of HSC in a cell-autonomous manner. However, they exert their role, not through interacting with *Cxcr3* or *Cxcl10* in the microenvironment. They may interact with other receptors or ligands on the surface of HSC or component cells of the bone marrow microenvironment to maintain the normal function of HSC. For example, GPR182, an atypical receptor of *Cxcl10*, was reported to be expressed by endothelial cells. The endothelium-specific loss of GPR182 led to a defect of the niche to support HSC homeostasis [11]. This is consistent with the impairment of HSC function by loss of *Cxcl10* we observed in the primary mice and the secondary recipients.

Mechanistically, the loss of *Cxcl10* leads to the decreased expression level of genes regulating the quiescence of HSCs. This is consistent with the cell cycle alterations we observed in the primary mice. Pathway genes in G0 and early G1 phases were downregulated in *Cxcl10*-deficient HSCs. In contrast, we only identified a few DEGs in primary *Cxcr3*$^{-/-}$ HSCs. This seems to be consistent with the mild reconstitution disadvantage in *Cxcr3*$^{-/-}$ recipient mice. To confirm this finding and gain more information about the potential mechanism responsible for the loss of *Cxcl10* and *Cxcr3* in regulating HSC function, further transcriptomic analysis of HSCs under stress should be pursued, including donor HSCs in primary and secondary recipients and those stressed HSCs after irradiation.

Considering the complexity of chemokines and their receptors, studies involving GPR182, *Cxcl9*, and *Cxcl11* in the regulation of HSC function are warranted. Both their cell-autonomous and non-autonomous roles should be examined in the future. Of note, the data in this study were obtained with knockout mice generated by CRISPR/Cas9. The expression of target genes should be validated at the protein level and off-target effects may exist. Knockout models of *Cxcl10* and *Cxcr3* generated with other targeting sequences or homologous recombination could affirm the findings of the HSC function alteration we observed.

Conclusions

We investigated both the cell-autonomous and cell-non-autonomous roles of *Cxcl10* and its receptor *Cxcr3* in HSC. Both *Cxcl10* and *Cxcr3* regulate self-renewal of HSC and *Cxcl10* plays a role in the regulation of lineage specification of HSC. Our findings increase our understanding of the roles of chemokine-chemokine receptors in regulating the function of HSC. Further exploration and validation of the underlying mechanisms through which the chemokines exert their regulatory roles in the HSCs is needed.

Abbreviations

HSC	Hematopoietic stem cell
HSPC	Hematopoietic stem and progenitor cell
LT-HSC	Long-term hematopoietic stem cell
Cxcl10	C-X-C motif chemokine ligand 10
Cxcr3	C-X-C motif chemokine receptor 3
LSK	Lin^- $Sca\text{-}1^+c\text{-}Kit^+$
ST-HSC	Short-term hematopoietic stem cell
MPP	Multipotent progenitor
DEGs	Differentially-expressed genes

Supplementary Information

The online version contains supplementary material available at https://doi.org/10.1186/s13287-024-03861-7.

Supplementary Material 1

Supplementary Material 2

Acknowledgements

Not applicable.

Author contributions

HZ and JD designed the study. FSL, XFS, SQD, YYW, XCL, CPW, KXH, YL, ZXD, WHX, MCL, ZYC, ZYJ, JX and JD performed experiments and analyzed the data. FSL and JD drafted the manuscript. HZ reviewed and edited the manuscript. HZ approved the final version of the manuscript.

Funding

This study was supported by the Talent Young Program of Guangdong Province (2021B1515020017), and the National Natural Science Foundation of China (Grant No. 81970143 and No. 82270167) to HZ.

Data availability

All the fastq raw data files of RNA-seq included in this study have been uploaded to the Gene Expression Omnibus (GEO) database (GSE272747) and will be publicly available from Jul 25, 2024. The authors confirm the availability of supporting data within this article and its supplemental information.

Declarations

Ethical approval

The animal study protocols were approved by the Institutional Animal Care and Use Committee (IACUC) of JINAN University under multiple approved proposals and listed below. 1."CXCR3 regulates survival and self-renewal of hematopoietic stem/progenitor cells"This study was approved on April 25, 2021, with approval number IACUC: 20210425-03. 2."CXCL10 regulates survival and self-renewal of hematopoietic stem/progenitor cells"This study was approved on April 25, 2021, with approval number IACUC: 20210425-04. 3."CXCL10 -CXCR3- CXCL9 regulate survival and self-renewal of hematopoietic stem/progenitor cells". This study was approved on April 29, 2021, with approval number IACUC: 20210429-13. 4. "CXCL10, CXCR3, CXCL9 regulate survival and self-renewal of hematopoietic stem/progenitor cells [2]". This study was approved on June 4, 2021, with approval number IACUC: 20210607-04. 5."CXCL10 and CXCR3 regulate hematopoietic stem progenitor cell differentiation and self-renewal". This study was approved on October 22, 2021, with approval number IACUC: 20211022-010. All animal experiments were performed according to the National Institutes of Health guide for the care and use of laboratory animals on ethics.

Consent for publication

Not applicable.

Competing interests

The authors declare no competing interests.

Received: 16 August 2023 / Accepted: 28 July 2024
Published online: 07 August 2024

References

1. Chen Z, Guo Q, Song G, Hou Y. Molecular regulation of hematopoietic stem cell quiescence. Cell Mol Life Sci. 2022;79(4):218.
2. Pinho S, Frenette PS. Haematopoietic stem cell activity and interactions with the niche. Nat Rev Mol Cell Biol. 2019;20(5):303–20.
3. Crane GM, Jeffery E, Morrison SJ. Adult haematopoietic stem cell niches. Nat Rev Immunol. 2017;17(9):573–90.
4. Griffith JW, Sokol CL, Luster AD. Chemokines and chemokine receptors: positioning cells for host defense and immunity. Annu Rev Immunol. 2014;32:659–702.
5. Schulz O, Hammerschmidt SI, Moschovakis GL, Förster R. Chemokines and chemokine receptors in lymphoid tissue Dynamics. Annu Rev Immunol. 2016;34:203–42.
6. Bonavita O, Mollica Poeta V, Massara M, Mantovani A, Bonecchi R. Regulation of hematopoiesis by the chemokine system. Cytokine. 2018;109:76–80.

7. Sugiyama T, Kohara H, Noda M, Nagasawa T. Maintenance of the hematopoietic stem cell pool by CXCL12-CXCR4 chemokine signaling in bone marrow stromal cell niches. Immunity. 2006;25(6):977–88.
8. Tisdale JF, Pierciey FJ Jr., Bonner M, Thompson AA, Krishnamurti L, Mapara MY, et al. Safety and feasibility of hematopoietic progenitor stem cell collection by mobilization with plerixafor followed by apheresis vs bone marrow harvest in patients with sickle cell disease in the multi-center HGB-206 trial. Am J Hematol. 2020;95(9):E239–42.
9. Shah H, Kim S, Singh P, Alavi A, Ratanatharathorn V, Ayash L, et al. Clinical outcomes of multiple myeloma patients who undergo autologous hematopoietic stem cell transplant with G-CSF or G-CSF and plerixafor mobilized grafts. Am J Hematol. 2020;95(2):198–204.
10. Zhang J, Supakorndej T, Krambs JR, Rao M, Abou-Ezzi G, Ye RY, et al. Bone marrow dendritic cells regulate hematopoietic stem/progenitor cell trafficking. J Clin Investig. 2019;129(7):2920–31.
11. Le Mercier A, Bonnavion R, Yu W, Alnouri MW, Ramas S, Zhang Y et al. GPR182 is an endothelium-specific atypical chemokine receptor that maintains hematopoietic stem cell homeostasis. Proc Natl Acad Sci USA. 2021;118(17).
12. Sinclair A, Park L, Shah M, Drotar M, Calaminus S, Hopcroft LE, et al. CXCR2 and CXCL4 regulate survival and self-renewal of hematopoietic stem/progenitor cells. Blood. 2016;128(3):371–83.
13. Graham SM, Vass JK, Holyoake TL, Graham GJ. Transcriptional analysis of quiescent and proliferating CD34 + human hemopoietic cells from normal and chronic myeloid leukemia sources. Stem Cells. 2007;25(12):3111–20.
14. Kim D, Langmead B, Salzberg SL. HISAT: a fast spliced aligner with low memory requirements. Nat Methods. 2015;12(4):357–60.
15. Li B, Dewey CN. RSEM: accurate transcript quantification from RNA-Seq data with or without a reference genome. BMC Bioinformatics. 2011;12:323.

Publisher's Note